

Article

Nitric Oxide Increases the Physiological and Biochemical Stability of Soybean Plants under High Temperature

Roberto Gomes Vital ¹, Caroline Müller ¹, Fábila Barbosa da Silva ², Priscila Ferreira Batista ¹, Andrew Merchant ³, David Fuentes ³, Arthur Almeida Rodrigues ⁴ and Alan Carlos Costa ^{1,*}

¹ Ecophysiology and Plant Productivity Laboratory, Goiano Federal Institute of Science and Technology–Campus Rio Verde, P.O. Box 66, Rio Verde 75901-970, GO, Brazil

² Stressed Plant Studies Laboratory, The University of São Paulo, Luiz de Queiroz College of Agriculture (ESALQ), P.O. Box 9, Piracicaba 13418-900, SP, Brazil

³ Centre for Carbon Water and Food, The University of Sydney, 380 Werombi road, Camden, 2570 NSW, Australia

⁴ Plant Anatomy Laboratory, Goiano Federal Institute of Science and Technology–Campus Rio Verde, P.O. Box 66, Rio Verde 75901-970, GO, Brazil

* Correspondence: alcarcos@gmail.com; Tel.: +55-643-620-5617; Fax: +55-643-620-5640

Received: 3 July 2019; Accepted: 24 July 2019; Published: 26 July 2019



Abstract: Thermal stress reduces plant growth and development, resulting in considerable economic losses in crops such as soybeans. Nitric oxide (NO) in plants is associated with tolerance to various abiotic stresses. Nevertheless, there are few studies of the range of observed effects of NO in modulating physiological and metabolic functions in soybean plants under high temperature. In the present study, we investigated the effects of sodium nitroprusside (SNP, NO donor), on anatomical, physiological, biochemical, and metabolic processes of soybean plants exposed to high temperature. Soybean plants were grown in soil: sand (2:1) substrate in acclimatized growth chambers. At developmental V3 stage, plants were exposed to two temperatures (25 °C and 40 °C) and SNP (0 and 100 µM), in a randomized block experimental design, with five replicates. After six days, we quantified NO concentration, leaf anatomy, gas exchange, chlorophyll *a* fluorescence, photosynthetic pigments, lipid peroxidation, antioxidant enzyme activity, and metabolite profiles. Higher NO concentration in soybean plants exposed to high temperature and SNP showed increased effective quantum yields of photosystem II (PSII) and photochemical dissipation, thereby maintaining the photosynthetic rate. Under high temperature, NO also promoted greater activity of ascorbate peroxidase and peroxidase activity, avoiding lipid peroxidation of cell membranes, in addition to regulating amino acid and organic compound levels. These results suggest that NO prevented damage caused by high temperature in soybean plants, illustrating the potential to mitigate thermal stress in cultivated plants.

Keywords: antioxidant system; metabolites; photosynthetic efficiency; sodium nitroprusside; soybean; thermo tolerance

1. Introduction

Soybean (*Glycine max* (L.) Merrill) is one of the most economically important crops worldwide. Soybeans are used for both human and animal foods, as well as for biodiesel production. The plant grows in tropical and subtropical environments and is susceptible to more frequent heat waves that result from climate change, compromising crop development and yields [1]. Heat waves are characterized by short periods with temperatures up to 6 °C above the average recorded temperature [2]. Changes in frequency, duration, and intensity of heat events are expected to increase in the context

of climate change; current projections suggest increased average global temperatures of 2 °C by 2050 [3]. These climatic changes threaten not only food security but also economic security for soybean producing countries [4].

For plants, thermal stress is characterized by increased temperature sufficient to alter leaves and affect metabolism [5]; in soybeans, this results in lower yields [6]. For each degree of increased mean temperature, soybean yield decreases by 16% [7]. Generally speaking, higher temperatures cause decreased photosynthetic rates because of several physiological and biochemical factors, including increased RuBisCO-mediated photorespiration [8]; this is followed by increased starch and soluble carbohydrate metabolism, leading to reduced availability of organic substrates and compromised plant development [8].

Exogenous application of signaling molecules can potentially improve the adaptability of plants under conditions of environmental stress. Nitric oxide (NO) regulates growth and development processes, including mitigating damage caused by high temperature in beans [9] and wheat [10]. Chen et al. [11] reported photosynthetic recovery in tall fescue exposed at 44 °C after application of sodium nitroprusside (SNP, NO donor). This effect is attributable to NO involvement in several physiological and biochemical processes of plants influencing stomata function [12], as well as stimulation of antioxidant responses [13].

Although some studies described the role of NO in photosynthetic or oxidative characteristics in different plants exposed to high temperature combined with different abiotic stresses [10,11,14,15], there is still a lack of understanding NO interactions modulating the physiological, biochemical, metabolic, and anatomical changes under thermal stress in the soybean. Therefore, in this study, we tested the hypothesis that NO would increase the tolerance of soybean plants to thermal stress, by maintaining metabolic homeostasis.

2. Materials and Methods

2.1. Experimental Conditions and Experimental Design

Plants were grown and measured in growth chambers (Instalafrio, Pinhais, PR, Brazil) with controlled conditions of relative humidity (~65%), irradiance (~650 $\mu\text{mol}\cdot\text{m}^{-2}\cdot\text{s}^{-1}$) and temperature (25/20 °C or 40/25 °C, day/night) at the Ecophysiology and Plant Productivity Laboratory at the Goiano Federal Institute of Education, Science and Technology (IF Goiano), Rio Verde Campus. Soybean plants (*Glycine max* (L.) Merrill), cultivar Desafio 8473 RSF (Brasmax Sementes, Cambé, PR, Brazil), were grown in polyethylene pots containing 5 kg of substrate prepared from Red Latosol (LVdf) soil and sand (2:1). The substrate used had the following composition: pH CaCl₂—5.6; P—0.7 $\text{mg}\cdot\text{dm}^{-3}$; K—13.0 $\text{mg}\cdot\text{dm}^{-3}$; Ca—1.54 $\text{cmol}_c\cdot\text{dm}^{-3}$; Mg—0.22 $\text{cmol}_c\cdot\text{dm}^{-3}$; Al—0.05 $\text{cmol}_c\cdot\text{dm}^{-3}$; H⁺ Al—1.3 $\text{cmol}_c\cdot\text{dm}^{-3}$; S—3.5 $\text{mg}\cdot\text{dm}^{-3}$; B—0.8 $\text{mg}\cdot\text{dm}^{-3}$; Cu—1.0 $\text{mg}\cdot\text{dm}^{-3}$; Fe—37.8 $\text{mg}\cdot\text{dm}^{-3}$; Mn—13.2 $\text{mg}\cdot\text{dm}^{-3}$; Zn—0.1 $\text{mg}\cdot\text{dm}^{-3}$; Na—6.0 $\text{mg}\cdot\text{dm}^{-3}$; SB—58%; CTC—3.1 $\text{cmol}_c\cdot\text{dm}^{-3}$; organic matter—109%. Based on these characteristics, liming was performed using dolomitic limestone, increasing the base saturation to 60%. The plants were fertilized with 0.2 $\text{g}\cdot\text{dm}^{-3}$ mono-ammonium phosphate (MAP), 0.16 $\text{g}\cdot\text{dm}^{-3}$ potassium chloride (KCl), 0.18 $\text{g}\cdot\text{dm}^{-3}$ potassium sulphate (K₂SO₄), 0.2 $\text{g}\cdot\text{dm}^{-3}$ urea (CH₄N₂O), and 0.026 $\text{g}\cdot\text{dm}^{-3}$ zinc sulfate (ZnSO₄), according to the recommendation for Cerrado soils [16]. Two plants were grown per pot, representing one experimental unit.

Treatments consisted of a combination of an aqueous solution of sodium nitroprusside (SNP, NO donor; Na² [Fe (CN)₅ NO]·2H₂O, SigmaAldrich, Saint Louis, MO, USA) and elevated temperature imposed at the V3 development stage [17]. The plants were treated with two doses of SNP: 0 and 100 μM for two consecutive days at 24-h intervals, using a hand sprayer with a total volume of 5 mL per plant [18], under 25 °C and 40 °C. The high temperature (HT) was imposed after the both SNP applications by gradually increasing from 25 °C at 10:00 a.m. until reaching 40 °C \pm 0.5 °C at 11:30 a.m., which was maintained for five hours. After this period, the temperature gradually decreased until it returned to 25 °C at 6:30 p.m., until repeating the cycle the following day. Thermal

treatments were imposed for a six-day period, during which time physiological, biochemical, metabolic, and morphoanatomical evaluations were made.

The experimental design was in randomized blocks, in a factorial scheme, with two SNP levels (0 and 100 μM) and two temperatures (25 °C and 40 °C), with five replicates.

2.2. Nitric Oxide Concentration

Endogenous NO concentration was determined according to Zhou et al. [19]. Briefly, fresh leaves (~2 g) were ground in 1.5 mL of acetic acid buffer (50 mM) containing zinc diacetate (4%), pH 3.6. The homogenates were centrifuged at 10,000 \times g for 15 min at 4 °C. The supernatant was collected. The pellet was washed with 1 mL of extraction buffer and the supernatant collected and combined. The samples were mixed and filtered and the extract (1 mL) was added to an equal volume of the Griess reagent. The samples were incubated at room temperature for 30 min and then the absorbance was determined at 540 nm using an ultraviolet-visible light (UV-Vis) spectrophotometer (Evolution 60S, Thermo Fisher Scientific, Madison, WI, USA). NO content was determined by comparison with a NaNO_2 standard curve (0 to 120 $\mu\text{g}\cdot\text{mL}^{-1}$) and was expressed as $\text{nmol}\cdot\text{g}^{-1}$ fresh weight (FW).

2.3. Photosynthetic Pigments, Gas Exchange, and Chlorophyll *a* Fluorescence

Photosynthetic pigments were extracted from leaf discs (~2 cm^2) in 5 mL of dimethylsulfoxide solution saturated with calcium carbonate in a 65 °C water bath. After 24 h, the solution absorbance was read at 480, 649.1, and 665.1 nm using a UV-Vis spectrophotometer. Chlorophyll *a* ($\text{Chla} = 12.4\cdot A_{665.1} - 3.62\cdot A_{649.1}$), chlorophyll *b* ($\text{Chlb} = 25.06\cdot A_{649.1} - 6.50\cdot A_{665.1}$) and total carotenoid ($\text{Carot} = [1000\cdot A_{480} - 1.29\cdot \text{Ca} - 53,78\cdot \text{Cb}]/220$) concentrations were calculated according to Wellburn [20] and were expressed as $\mu\text{g}\cdot\text{cm}^{-2}$.

Gas exchange was measured in fully expanded leaves using an infrared gas analyzer (IRGA, LI-6400xt, Licor, Lincoln, NE, USA) to determine the net photosynthetic assimilation rate (A , $\mu\text{mol}\cdot\text{m}^{-2}\cdot\text{s}^{-1}$), stomatal conductance (g_s , $\text{mmol}\cdot\text{m}^{-2}\cdot\text{s}^{-1}$), transpiration rate (E , $\text{mmol}\cdot\text{m}^{-2}\cdot\text{s}^{-1}$), and the ratio of internal to external CO_2 (C_i/C_a). Measurements were performed under constant photosynthetically active radiation (PAR, 1000 $\mu\text{mol}\cdot\text{m}^{-2}\cdot\text{s}^{-1}$), and at environmental atmospheric CO_2 concentration (C_a) (~430 $\mu\text{mol}\cdot\text{mol}^{-1}$), temperature (~25 °C) and relative air humidity (4–65%), between 8:00 a.m. and 10:00 a.m.

Chlorophyll *a* fluorescence images and values were obtained using a modulated fluorometer (Imaging-PAM, Heinz Walz, Effeltrich, BY, Germany). The fluorescence signals of the leaf area examined were captured using a charge-coupled device (CCD) camera coupled to the device images. The pixel-value images of the fluorescence variables were displayed using a false color code ranging from black (0.000) to pink (1.000). To obtain measurements, leaves were initially dark-acclimated for 40 min so that the reaction centers were fully opened to obtain the minimal (F_0) and maximal chlorophyll fluorescence (F_m) values. From measurements, the maximum photochemical efficiency photosystem II (PSII) ($F_v/F_m = (F_m - F_0)/F_m$) was calculated. The leaf tissues were then exposed to actinic light and a saturating pulse to obtain the steady-state fluorescence (F) and the maximum fluorescence in a light-adapted state (F_m'), respectively. This allowed determination of the effective quantum yield of PSII ($Y_{II} = (F_m' - F)/F_m'$), quenching photochemical ($qP = (F_m' - F)/(F_m' - F_0)$) and the quantum yield of regulated energy dissipation ($Y_{NPQ} = (F/F_m') - (F/F_m)$). The Y_{II} was used to calculate the electron transport rate, $ETR = Y_{II}\cdot\text{PAR}\cdot\text{Leaf}_{\text{ABS}}\cdot 0.5$, where PAR is the photon flow ($\mu\text{mol}\cdot\text{m}^{-2}\cdot\text{s}^{-1}$) on the leaves, Leaf_{ABS} is the fraction of incident light that is absorbed by the leaves, and 0.5 is the excitation energy fraction directed to the PSII.

2.4. Leaf Morphoanatomical Characterization

Samples (~3 cm^2) from the middle region of the last fully expanded leaf were collected and fixed in Karnofsky solution. After 24 h, the material was pre-washed in phosphate buffer and dehydrated in a gradual ethyl alcohol series, pre-filtered, and infiltrated in historesin (Leica, Wetzlar, HE, Germany),

according to the manufacturer's recommendation. Samples were then transversely sectioned to 5- μm thickness in a rotating microtome (1508R model, Logen Scientific, Shangjiao Dashi, Guangzhou, China). Sections were stained with toluidine blue (0.05% in 0.1 M phosphate buffer, pH 6.8) and anatomical observations of adaxial and abaxial epidermis, palisade, and spongy parenchyma and mesophyll were made using images photographed with an Olympus microscope (BX61, Olympus, Shinjuku-ku, Japan) coupled to a DP-72 camera using the light-field option. The micromorphometry measurements were obtained from the previous images using ImageJ software (Image Processing and Analysis in Java, v. 1.47, Bethesda, MD, USA). Ten observations per replicate were measured for each structure evaluated.

2.5. Lipid Peroxidation and Antioxidant Enzyme Activities

Lipid peroxidation levels were measured as malondialdehyde (MDA) content, according to Heath and Packer [21]. Leaf samples (~0.160 g) were homogenized in 2 mL of trichloroacetic acid (TCA, 1%, and centrifuged at $12,000\times g$ for 15 min at 4 °C. The supernatant (500 μL) was mixed with 2 mL of thiobarbituric acid (TBA) reagent (0.5% TBA in 20% TCA), heated at 95 °C for 20 min in water bath and then quickly cooled in an ice bath and centrifuged at $3000\times g$ for 4 min. The absorbance was measured at 440, 532, and 600 nm using a UV-Vis spectrophotometer. MDA concentration was calculated using the molar extinction coefficient of $155\text{ M}^{-1}\cdot\text{cm}^{-1}$, as $\text{MDA (nmol}\cdot\text{mL}^{-1}) = [((\text{Abs}_{532} - \text{Abs}_{600}) - (\text{Abs}_{440} - \text{Abs}_{600}))/155,000]10^6$, and expressed as $\text{nmol MDA}\cdot\text{g}^{-1}\text{ FW}$.

To determine the activities of superoxide dismutase (SOD), catalase (CAT), ascorbate peroxidase (APX), and peroxidase activity (POX), leaf tissues (~0.2 g) were ground into a fine powder in liquid nitrogen and homogenized in 2 mL of a solution containing 50 mM potassium phosphate buffer (pH 6.8), 0.1 mM ethylenediaminetetraacetic acid (EDTA), 1 mM phenylmethylsulfonyl fluoride (PMSF), and 2% polyvinylpolypyrrolidone (PVPP). The homogenates were centrifuged at $12,000\times g$ for 15 min at 4 °C, and the supernatants were used as a crude enzyme extract. SOD (EC 1.15.1.1) activity was determined by measuring the ability to photochemically reduce *p*-nitrotetrazole blue (NBT) according to Del Longo et al. [22]. The reaction was started by the addition of 10 μL of the crude enzyme extract to 280 μL of a mixture containing 50 mM potassium phosphate buffer (pH 7.8), 13 mM methionine, 0.075 mM NBT, 0.1 mM EDTA, and 0.002 mM riboflavin. The reaction occurred at 25 °C under a 15-W lamp. After 15 min of light exposure, the light was interrupted, and the production of formazan blue—which resulted from the photoreduction of NTB—was monitored by the increase in absorbance at 560 nm using a microplate reader (VersaMax, Molecular Devices, San Jose, CA, USA). Controls for each sample were obtained from aliquots maintained in the light during the reaction time. One SOD unit was defined as the amount of enzyme required to inhibit NBT photoreduction by 50%, and was expressed in $\text{U}\cdot\text{min}^{-1}\cdot\text{mg}^{-1}\text{ protein}$.

Catalase (EC 1.11.1.6) activity was assayed according to the method described by Havir and McHale [23]. The reaction consisted of 10 μL of the crude enzyme extract and 990 μL of a solution containing potassium phosphate buffer (100 mM; pH 6.8) and H_2O_2 (12.5 mM). The CAT activity was determined by the rate of H_2O_2 decomposition at 240 nm in UV-Vis spectrophotometer for 1.5 min at 25 °C. An extinction coefficient of $36\text{ M}^{-1}\cdot\text{cm}^{-1}$ was used to calculate the CAT activity, which was expressed as $\text{min}^{-1}\cdot\text{mg}^{-1}\text{ protein}$.

APX (EC 1.11.1.11) activity was determined according to Nakano and Asada [24]. The reaction consisted of 50 μL of the crude enzyme extract and 1.95 mL of reaction solution containing potassium phosphate buffer (50 mM; pH 6.0), H_2O_2 (1 mM), and ascorbate (0.8 mM). The APX activity was measured by the rate of ascorbate oxidation at 290 nm using a UV-Vis spectrophotometer for 3 min at 25 °C. An extinction coefficient of $0.0028\text{ M}^{-1}\cdot\text{cm}^{-1}$ was used to calculate the APX activity, which was expressed as $\mu\text{mol}\cdot\text{min}^{-1}\cdot\text{mg}^{-1}$ of protein.

Peroxidase (POX, EC 1.11.1.7) activity was determined according to Kar and Mishra [25]. The reaction consisted of 100 μL of the crude enzyme extract and 1.9 mL of a reaction mixture containing potassium phosphate buffer (25 mM; pH 6.8), pyrogallol (20 mM), and hydrogen peroxide (20 mM). The absorbance was measured at 420 nm in UV-Vis spectrophotometer for 1 min at

25 °C. An extinction coefficient of $0.00247 \text{ M}^{-1}\cdot\text{cm}^{-1}$ was used to calculate the POX activity, which was expressed as $\mu\text{mol}\cdot\text{min}^{-1}\cdot\text{mg}^{-1}$ of protein. Protein concentration was determined according to Bradford [26].

2.6. Metabolic Extraction and Analysis

The leaf samples were initially microwave dried (900 W) for 10 s to prevent metabolic turnover [27,28], and then approximately 40 mg of dried leaf material was extracted with 1 mL of methanol/chloroform/water (12:5:3, *v/v/v*) at 75 °C for 30 min. The water fraction of the extraction mixture consisted of a 0.1% solution of internal standard. The mixture of 0.1% penta-erythritol and 0.1% 3-nitrotyrosine for GC analysis.

Samples were centrifuged at $11,400\times g$ and 800 μL of the supernatants were collected and mixed to 200 μL chloroform and 500 μL of Milli-Q water to facilitate phase separation. Samples were then centrifuged at $11,400\times g$ for 3 min and 700 μL of the water–methanol-soluble fractions were collected and stored at $-20\text{ }^{\circ}\text{C}$ for further analysis.

Analysis of soluble carbohydrates, sugars, and organic acids were performed using GC on an Agilent 7890A gas chromatograph coupled to a 7000 QQQ Mass selective detector (Agilent, Santa Clara, CA, USA). A HP5 column (0.25 mm internal diameter, 30 m long, 0.25 μm film thickness) was used for chromatographic separation. Then, 50 μL of extract was dried down in a SpeedVac and derivatized using 450 μL of pyridine and 50 μL of *N,O*-bis(trimethylsilyl)trifluoroacetamide (BSTFA):trimethylchlorosilane (TMCS) (10:1) for derivatization to make up a final volume of 500 μL for GC–MS analysis. Samples were incubated for 35 min at 75 °C and analyzed by GC–MS within 24 h. A 20:1 split injection was made at 300 °C initial oven temperature program of 60 °C for 2 min, ramping to 220 °C at $10\text{ }^{\circ}\text{C}\cdot\text{min}^{-1}$ (hold for 5 min), then ramping at $10\text{ }^{\circ}\text{C}\cdot\text{min}^{-1}$ to 300 °C (hold for 5 min). Peak integration was made using Agilent MassHunter software (Agilent, Santa Clara, CA, USA). A mixed standard was made from a stock solution containing 500 $\mu\text{g}\cdot\text{mL}^{-1}$ of each analyte. Appropriate aliquots were taken to make standard concentrations of 0.5, 1, 5, 10, 20, and 50 $\mu\text{g}\cdot\text{mL}^{-1}$. The dry weight of the sample was used for the calculation and the results were expressed as $\mu\text{g}\cdot\text{g}^{-1}$ of dry weight.

Analysis of amino acids was performed using the underivatized extracts on a 1290 Infinity LC-MS system (Agilent, Santa Clara, CA, USA) coupled to a 6520 QTOF Mass selective detector (Agilent, Santa Clara, CA, USA). A 3.5- μL sample was injected into a Zorbax SB-C18 column (2.1 \times 150 mm, 3.5 μm), and separation was achieved by gradient elution with water and methanol. The quadrupole time-of-flight (QTOF) was tuned to operate at low-mass range ($<1700\text{ }m/z$), data acquisition was performed in scan mode (60–1700 m/z), and ionization performed in positive ion mode. LC–MS results were identified based on their retention times relative to standards, as well as their formula mass. Peaks were integrated and their relative quantities were calculated using MassHunter software. A mixed standard was made from a stock solution containing 500 $\mu\text{g}\cdot\text{mL}^{-1}$ of each analyte. The solutions were kept frozen at $-20\text{ }^{\circ}\text{C}$. Appropriate aliquots were taken to make resulting standard concentrations of 0.1, 0.2, 0.5, 1, 5, 10, and 20 $\mu\text{g}\cdot\text{mL}^{-1}$ into 1-mL solutions in Milli-Q Water. The dry weight of the sample was used for the calculation and the results were expressed as $\mu\text{g}\cdot\text{g}^{-1}$ of dry weight.

2.7. Statistical Analysis

The data were subjected to factorial analysis of variance ($p < 0.05$), and the means were compared using the Tukey test, using Analysis System Program Variance (SISVAR, v. 5.4, Lavras, MG, Brazil).

3. Results

3.1. Nitric Oxide Concentration

NO concentrations did not significantly differ in soybean plants at 25 °C. At 40 °C, SNP-treated plants showed a pronounced increase in NO concentration (Figure 1).

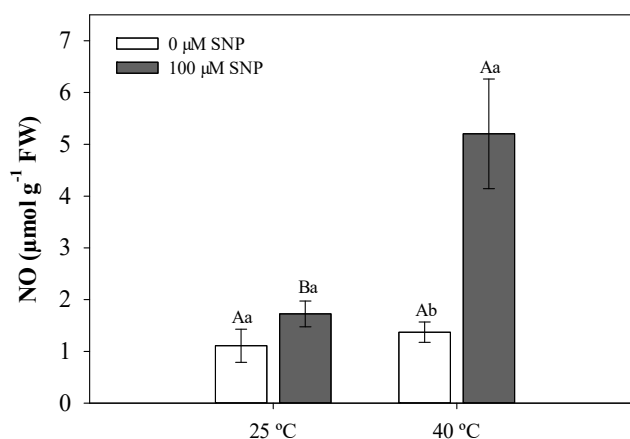


Figure 1. Nitric oxide (NO) content in soybean plants subjected to two temperatures (25 °C and 40 °C) and two sodium nitroprusside (SNP) concentrations (0 and 100 μM). Bars represent means ($n = 5$) \pm standard error (SE). Capital letters (between temperatures) and lowercase letters (within temperatures) represent significant differences using Tukey's test ($p < 0.05$).

3.2. Leaf Anatomical Traits

Transverse sections of soybean leaves showed epidermis cells varying in size and shape, generally tubular and rounded, in addition to being amphistomatic. Mesophyll (MS) cells were dorsiventral with two or three strata of palisade parenchyma (PP), whose cells ranged from less to more juxtaposed, and two or three spongy parenchyma (SP) strata with large intercellular spaces. Paravenous parenchyma (PvP) between the PP and SP were also present. The vascular bundle (VB) was surrounded by a sheath of parenchymal cells arranged in a juxtaposed position extending to the epidermis (Figure 2)

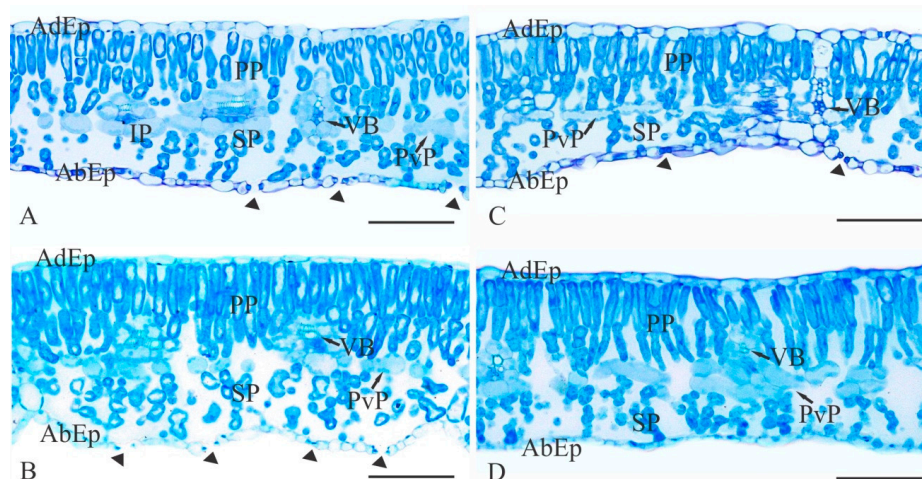


Figure 2. Cross-sectional photomicrographs of soybean leaf blades showing the mesophyll thickness after the treatments with temperature (°C) and SNP application (100 μM): **A**—25 °C; **B**—25 °C + SNP; **C**—40 °C; and **D**—40 °C + SNP. AdEp: adaxial epidermis; AbEp: abaxial epidermis; PP: palisade parenchyma; SP: spongy parenchyma; PvP: paravenous parenchyma; VB: vascular bundle. Arrowheads indicate stomata. Scale bars = 100 μm. For color version, the reader is referred to the web version of this article.

No significant differences were observed in the anatomical traits of soybean leaves exposed to 25 °C, independent of SNP application (Figure 3). In the high-temperature treatment group, a reduction in the PS portions was observed (Figure 3B) along with fewer intercellular spaces, causing decreased

MS (Figure 3C) and leaf thickness (Figure 3D). Soybean plants exposed to high temperature treated with SNP did not show anatomical changes compared to plants grown at 25 °C (Figure 3).

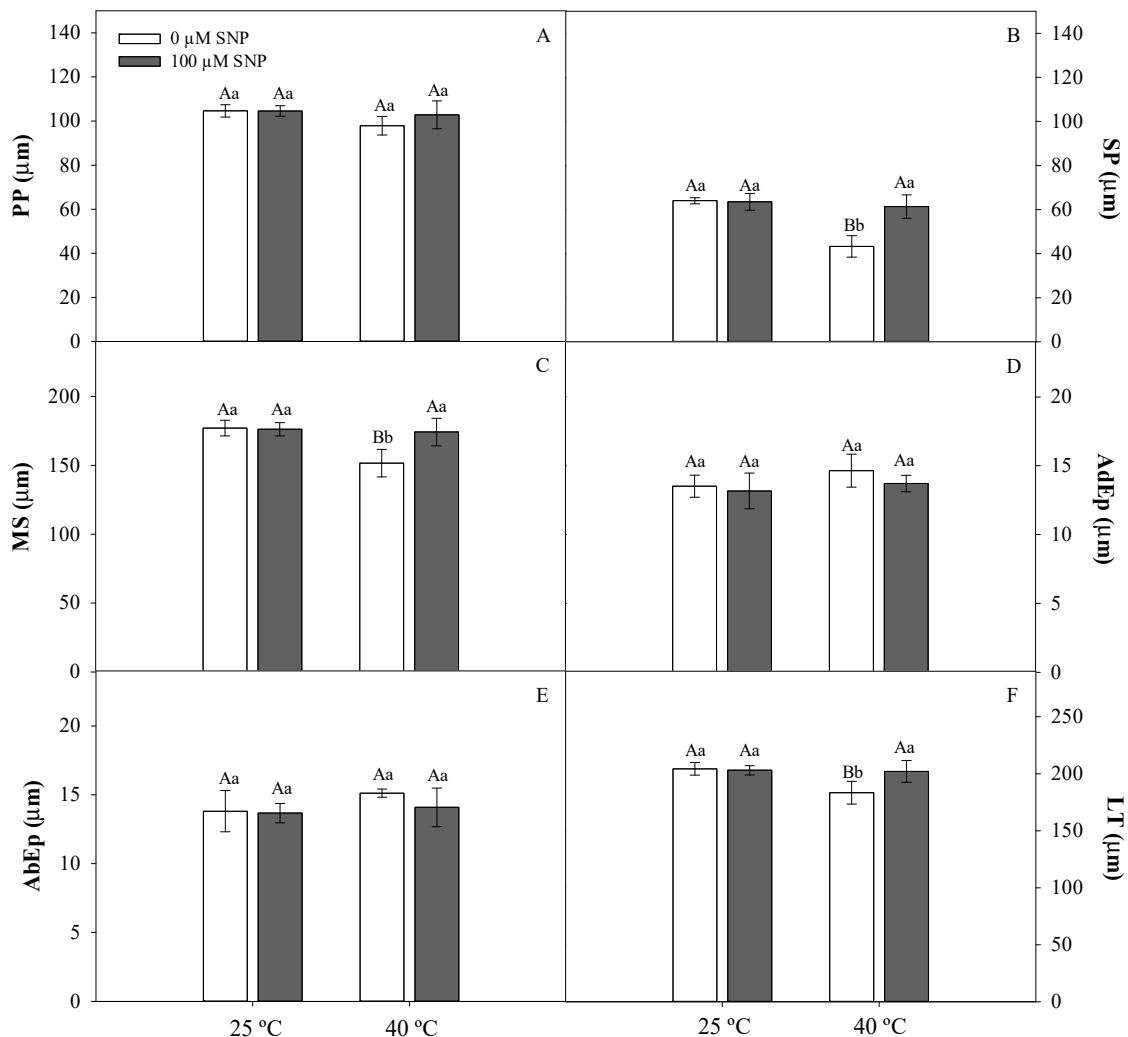


Figure 3. Palisade parenchyma (PP, A), spongy parenchyma (SP, B), mesophyll (MS, C), adaxial epidermis (AdEp, D), abaxial epidermis (AbEp, E), and leaf thickness (LT, F) in soybean plants submitted to two temperatures (25 °C and 40 °C) and two SNP concentrations (0 and 100 μM). Bars represent means ($n = 5$) \pm SE. Capital letters (between temperatures) and lowercase letters (within temperatures) represent significant differences using Tukey's test ($p < 0.05$).

3.3. Physiological Traits

No interactions were observed between the temperature and the application of SNP in terms of concentration of the photosynthetic pigments. High temperature and SNP application, as isolated factors, increased total chlorophyll (Chl $a + b$) content in soybean plants (data not shown). Carotenoid levels increased in plants cultivated at 40 °C, independent of SNP application (data not shown).

The photosynthetic rate was significantly lower in high-temperature-treated plants (Panel A); this was not observed in plants exposed to SNP and high temperature (Figure 4A). Stomatal conductance (g_s), transpiration rate (E), and the ratio between internal and external CO₂ concentration (C_i/C_a) were not significantly affected by temperature or SNP application (Figure 4B–D).

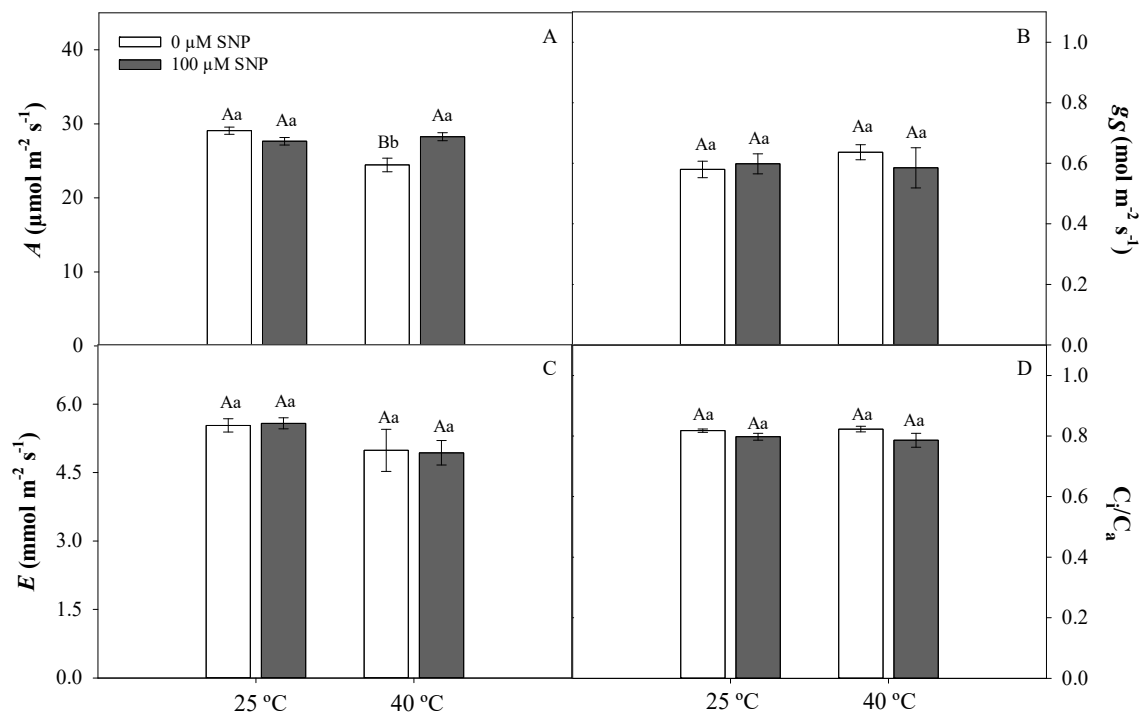


Figure 4. Photosynthetic rate (A , **A**), stomatal conductance (g_s , **B**), transpiratory rate (E , **C**), and ratio between internal and external CO_2 (C_i/C_a , **D**) in soybean plants submitted to two temperatures (25 °C and 40 °C) and two SNP concentrations (0 and 100 μM). Bars represent means ($n = 5$) \pm SE. Capital letters (between temperatures) and lowercase letters (within temperatures) represent significant differences using Tukey's test ($p < 0.05$).

High temperature caused an increase in the minimal fluorescence (F_0) and a decrease in the values of the effective quantum yield of PSII (Y_{II}), quenching photochemical (q_p) and electron transport rate (ETR) (Figure 5). The maximum photochemical efficiency of PSII (F_v/F_m) was not affected by high temperature (Figure 5). However, SNP application reversed the deleterious effects of high temperature, promoting an increase in Y_{II} and ETR. The quantum yield of regulated energy dissipation (Y_{NPQ}) was higher in high-temperature-treated plants and, at both temperatures, Y_{NPQ} was reduced by SNP application (Figure 5).

3.4. Antioxidant Defense System and Metabolic Profile of Soybean Plants

High temperature increased lipid peroxidation, as evidenced by higher MDA values (Figure 6). This observation was reversed in SNP-treated plants (Figure 6).

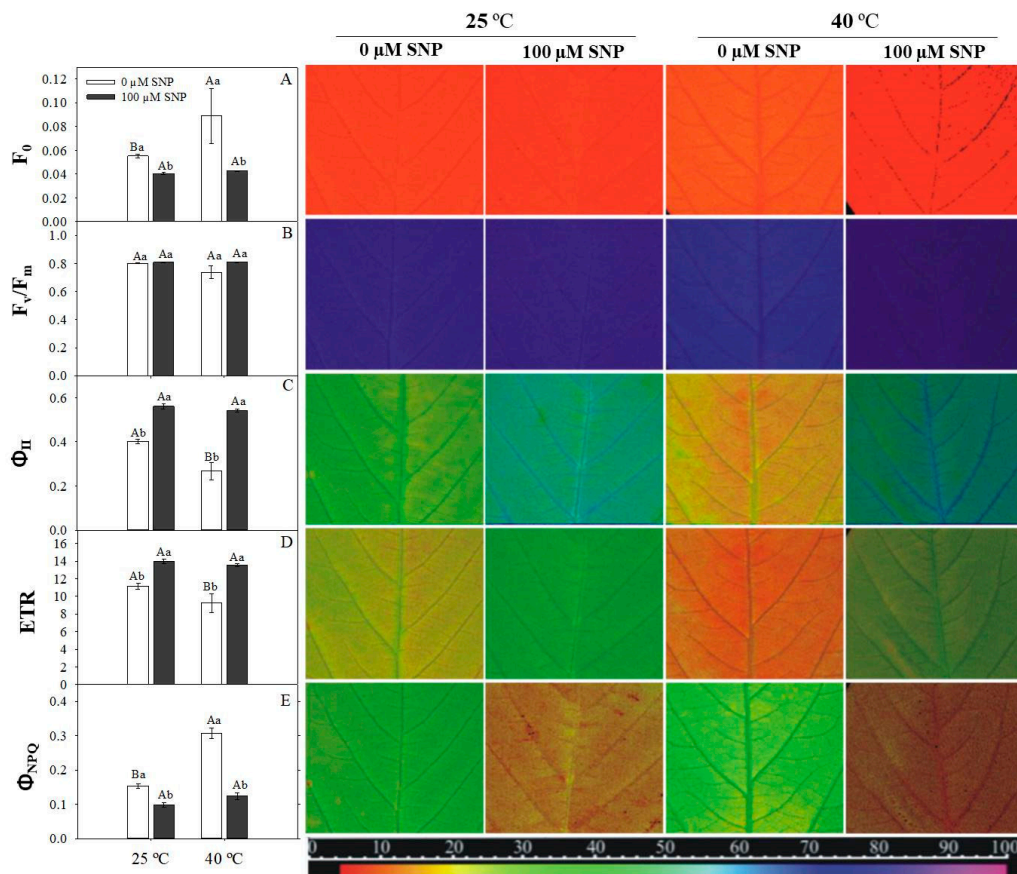


Figure 5. Minimal chlorophyll fluorescence (F_0 , **A**), maximum photosystem II (PSII) quantum yield (F_v/F_m , **B**), effective PSII quantum yield (Φ_{II} , **C**), apparent electron transport rate (ETR, **D**), and quantum yield of regulated energy dissipation (Φ_{NPQ} , **E**) in soybean plants submitted to two doses of SNP (0 and 100 μM) and two temperatures (25 °C and 40 °C). Bars represent means of five replicates \pm SE. Means followed by the same upper- and lowercase letters within the temperatures do not differ by the Tukey test ($p < 0.05$). The false color code depicted at the bottom of images ranges from 0 (black) to 100 (pink). For interpretation of the references to color in this figure legend, the reader is referred to the web version of this article.

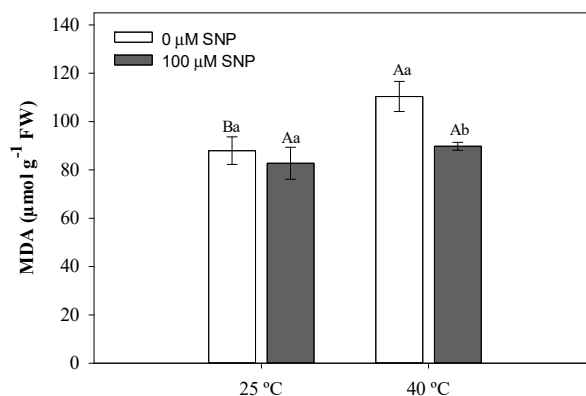


Figure 6. Malondialdehyde (MDA) concentration in soybean plants submitted to two temperatures (25 °C and 40 °C) and two SNP concentrations (0 and 100 μM). Bars represent means ($n = 5$) \pm SE. Capital letters (between temperatures) and lowercase letters (within temperatures) represent significant differences using Tukey's test ($p < 0.05$).

Antioxidant enzyme activity was significantly affected by at least one of the treatments imposed. Superoxide dismutase (SOD) and catalase (CAT) activities were higher in plants exposed only to high temperature; this was not observed in plants treated with high temperature and SNP (Figure 7A,B). The highest activities of ascorbate peroxidase (APX) and total peroxidases (POX) were observed in plants exposed to high temperature and SNP (Figure 7C,D).

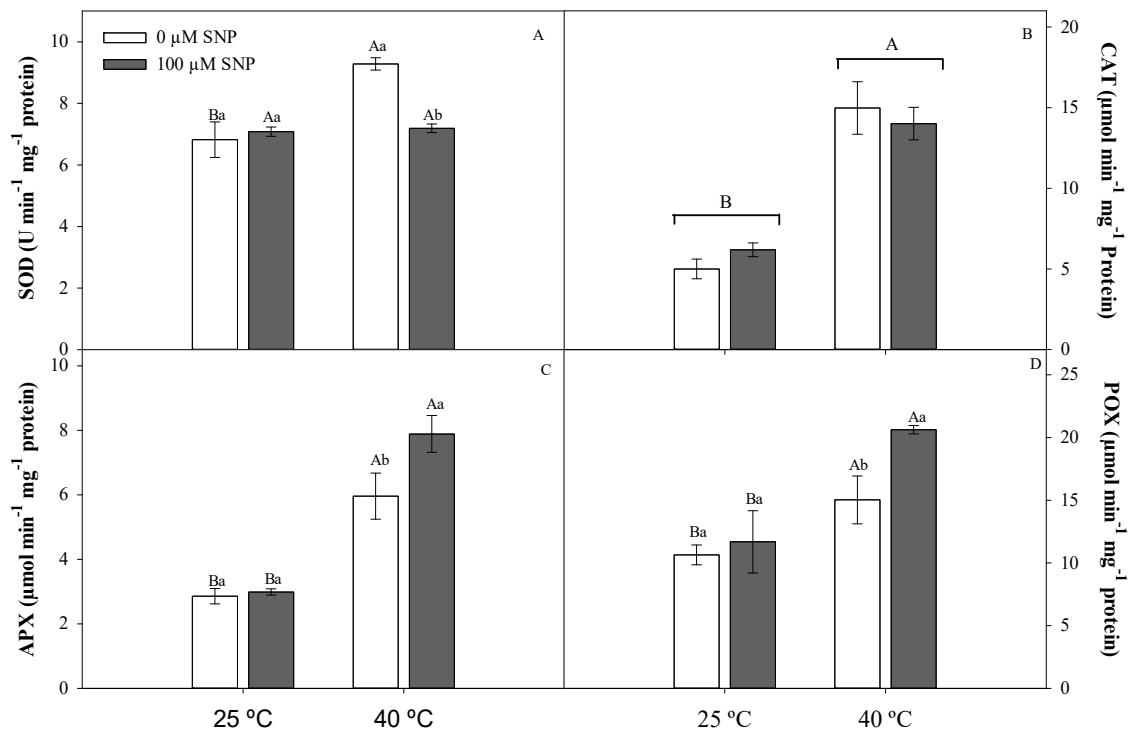


Figure 7. Dismutase superoxide (SOD, **A**), catalase (CAT, **B**), ascorbate peroxidase (APX, **C**), and total peroxidase (POX, **D**) activities in soybean plants submitted to two temperatures (25 °C and 40 °C) and two SNP concentrations (0 and 100 μM). Bars represent means ($n = 5$) \pm SE. Capital letters (between temperatures) and lowercase letters (within temperatures) represent significant differences using Tukey's test ($p < 0.05$).

3.5. Metabolic Profile of Soybean Plants

High temperature increased levels of tryptophan, phenylalanine tyrosine, histidine, and lysine when compared to 25 °C and 40 °C + SNP-treated plants (Figure 8 and Table S1, Supplementary Materials). SNP application reduced the levels of histidine, lysine, arginine, glycine, serine, alanine, aspartate, leucine, threonine, and isoleucine at 25 °C. The levels of glutamine, proline, and methionine were lower in the presence of NO, while asparagine and valine show higher levels only under high-temperature conditions.

SNP application promoted increased ribose and D-mannitol levels in plants exposed to high temperature. However, mannose levels were reduced in SNP-treated plants when compared to untreated SNP-plants under both temperatures. By contrast, increases in levels of pentaerythritol, citric acid, fructose, pinitol, glucose, and chiro-inositol were observed only with high temperature. SNP also reduced aminobutyric acid and chiro-inositol levels (Figure 8 and Table S2, Supplementary Materials).

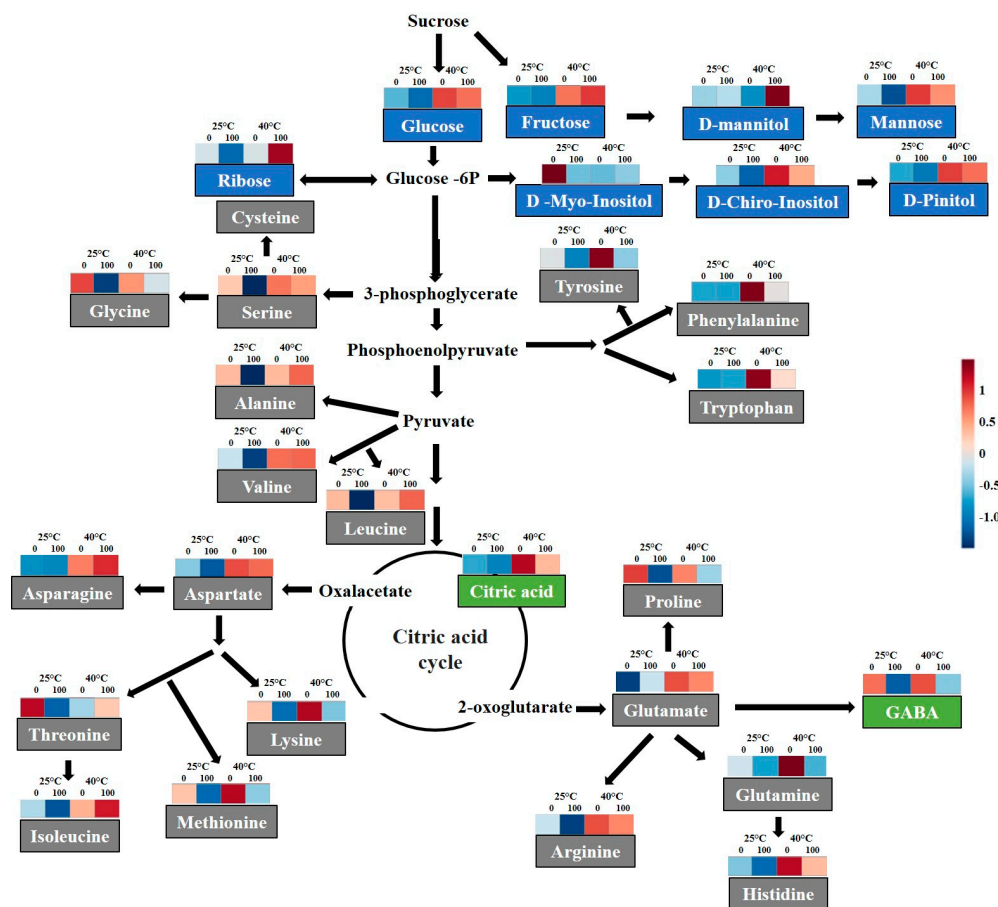


Figure 8. Schematic representation of the selected metabolic pathways with heat map of normalized compounds data integrated from soybean plants submitted to two temperatures (25 °C and 40 °C) and two SNP concentrations (0 and 100 μ M). Blue and red colors represent low and high concentrations, respectively, and scale according to the color legend. For interpretation of the references to color in this figure legend, the reader is referred to the web version of this article.

4. Discussion

Nitric oxide, through SNP application, increased the tolerance of soybean plants to thermal stress. NO was shown to improve the performance of cultivated plants exposed to various abiotic stresses, including water deficit [13,27,28] and salinity [29], suggesting that nitric oxide synthesis is regulated by genes that are upregulated under stress conditions [11,30]. Furthermore, it was shown that the activity of this uncharged molecule is easily transported across membranes, allowing rapid activation of cell signaling [31], changes in gene expression, and regulation of physiological processes [32] that are responsible for increasing thermal stress tolerance.

Damage to the spongy parenchyma and mesophyll thickness was observed in soybean leaves exposed to HT. This resulted in increased plasma membrane permeability and cellular leakage content as also observed in *Vitis vinifera* L. subjected to thermal stress [33]. However, the slight increase in mesophyll thickness and cell preservation in SNP-treated plants may be an adaptive characteristic of stress tolerance [34]. In the present study, we detected no changes in photosynthetic pigments under HT. Anatomical changes observed in the mesophyll cells probably limited CO₂ supply to RuBisCO, resulting in a lower photosynthetic rate in soybean plants. SNP application also increased the chlorophyll content in soybean plants. NO was shown to interact with metallo-group molecules, altering their stability, synthesis, and/or degradation rates [35], largely because chlorophyll molecules possess an Mg²⁺ atom in the porphyrin groups, a target for NO interactions [36]. These interactions may have led to the improved photosynthetic performance of soybean plants under high temperature.

The improvement of *A* may be related to an influence of NO on the activity of RuBisCO activase, as observed in rice growth under thermal stress [15]. By contrast, Hayat et al. [37] showed that NO application induced an increase in carbonic anhydrase, catalyzing the conversion of CO₂ into HCO₃⁻ and maintaining the CO₂ supply to RuBisCO.

HT promotes changes in the photochemical efficiency in soybean, as observed by an increase in minimal fluorescence (*F*₀) and reduction in energy efficiency in the electron transport photoefficiency rate (*Y*_{II} and ETR). Similar results were reported in tall fescue [11] and rice [15] subjected to HT. The increase in *F*₀ is associated with the centers' reactivity, complex antenna damage, or with increases in the distance between the protein structures that compose the PSII reaction center and the antenna complex, resulting in lower energy transfer to PSII. These changes occur mainly as a function of the highly unsaturated composition of the thylakoid membrane and the presence of temperature-sensitive photosystems [38]. During thermal stress, thylakoids are susceptible to loss of stacking and swelling of the granules, inducing photooxidative stress, reduction of PSII activity, and changes in electron transport for photosynthesis [39].

By contrast to the deleterious effects of HT, NO elicited an improvement in the chlorophyll *a* fluorescence in soybean plants. Increases in *Y*_{II} and ETR suggest that NO acted as a thermal stress reliever by improving electron transport chain stability and the higher conversion of light energy to chemical energy efficiency [14]. NO induces protein repair, and de novo synthesis of genes related to the photosystem (*psbA*, *psbB*) and the antenna complex (*psbC*, CP₄₇) under stress conditions [11,30]. Under high temperature only, the increase in carotenoid content and *Y*_{NPQ} acts as the first line of defense against the effects of stress conditions by activating photoprotective mechanisms, including the heat dissipation of excess energy [40], to avoid reactive oxygen species (ROS) formation and consequent PSII photoinhibition [15]. However, when excess energy dissipation is not sufficient to reduce PSII excitation pressure, ROS form and other suppression pathways may be required for their elimination, including the antioxidant enzyme system activation in an attempt to avoid cell damage. In our study, SNP-treated plants did not activate these mechanisms after six treatment days. The improvement of the photochemical efficiency of SNP-treated plants and the high photosynthetic rate suggest that the electrons were used in the photochemical pathway, avoiding oxidative damage by ROS production, as was observed in *Crambe abyssinica* Hochst. plants under water-deficit conditions [27,28].

Severe high temperatures promoted structural and functional changes in chloroplasts as a result of the oxidation of thylakoid membranes and proteins [41], as was observed by increases in MDA levels in maize, rice [42], and soybean plants. NO, on the other hand, reduced the photooxidative damage in SNP-treated plants at 40 °C. This protective effect may have occurred because of the ability of NO to react directly with ROS, by forming peroxynitrite (ONOO⁻), which is less toxic than H₂O₂ [43], or by inhibiting NADPH oxidase and reducing ROS production [44].

The abundance of amino acids, sugars, and sugar-alcohol levels suggests several important strategies for coping with thermal stress, because these molecules act as signaling agents [45]. Among the amino acids related to the maintenance of cellular metabolism, increases in the levels of tryptophan, phenylalanine, tyrosine, histidine, lysine, valine, and asparagine are likely related to defense responses in soybean plants under HT. Specifically, aromatic amino acids (tryptophan, phenylalanine, and tyrosine) are synthesized in the shikimic acid pathway, and are involved in the production of compounds that are important for cellular homeostasis, including phenolic compounds, electron transporters, enzyme cofactors, and antioxidant molecules [46]. These molecules were previously found in plants in response to thermal stress [47]. Furthermore, small amino acids such as valine can serve as osmoregulators [48] or may be used as sources of energy for the plant during stress [49].

Increased levels of the amino-acid asparagine may have occurred as a consequence of the increase in protein degradation that induces ammonium accumulation [50]. Under these conditions, increased asparagine synthesis prevents ammonium toxicity in the cells and regulates nitrogen levels, as reported in sunflower plants exposed to several abiotic stresses [51]. Therefore, the results of this study suggest

that increased levels of these amino acids maintain metabolic processes and prevent damage to cells through thermal stress, including loss of membrane integrity and denaturation of enzymes and proteins.

By contrast, the observed reduction in amino-acid levels in soybean plants, both at 25 °C and at 40 °C + SNP, raises further hypotheses. The first may be related to changes in nitrogen metabolism. The synthesis, reserve, and transport of amino acids depend on nitrogen distribution, regulated at the transcriptional level [52]. In this way, NO application may augment the nitrogen supply for nitrogen metabolism, thereby reflecting the constitutive accumulation of nitrogen to avoid future deficits. Regulation of amino-acid levels could participate in signaling and production of other metabolites [53], including polyamines. León et al. [54] observed extensive metabolic and transient reprogramming 6 h after treatment with NO in *Arabidopsis thaliana* (L.) Heynh, including increased polyamines levels that are considered good indicators of NO activation processes, dedicated to remedy oxidative stress and regulate plant growth and development. A second hypothesis may be associated not with decreased synthesis of these amino acids, but with reduction of protein degradation, resulting in lower concentrations of free amino acids. In this case, NO would have a protective role for these proteins by influencing plant metabolism, mainly under thermal stress. NO interacts with proteins through S-nitrosylation of cysteine residues [55]. This S-nitrosylation was associated with the regulation of plant growth and development processes as well as responses to environmental stimuli [56]. In *A. thaliana*, Iglesias et al. [57] observed that NO, through S-nitrosylation, regulated TIR1 and ASK1 proteins that act directly on the ubiquitin proteasome process in plants. According to these authors, the ubiquitin proteasome is the main mechanism for protein catabolism, as well as being part of the auxin co-receptor subunit during plant growth and development. Furthermore, in response to high temperature, S-nitrosylation regulates the activity of a molecular chaperone to Hsp90 that promotes folding and stabilization of hundreds of proteins [58].

NO application in soybean plants under HT demonstrated a potential role in the greater regulation of sugar levels of ribose and polyol D-mannitol. Increased concentration of sugars may assist in reducing heat-induced membrane rupture and consequent cellular leakage. Many sugar molecules help stabilize the lipid membrane via hydrogen-bonding interactions between sugar OH-groups and the lipid headgroups, avoiding phase transitions that may result in extravasation of solutes [59]. In addition, sugar-alcohols such as D-mannitol, in addition to acting on osmotic adjustment, have important antioxidant characteristics such as hydroxyl radical elimination, as observed for salinity in exposed corn plants [60]. In soybean plants exposed only to HT, increased levels of soluble sugars fructose and glucose are likely related to the degradation of sucrose and metabolic demand during defense responses during stress [61].

In conclusion, we found that SNP, an NO donor, played a significant role in mitigating the damaging conditions imparted by thermal stress in soybean plants. NO produced a relative improvement in physiological (increased *A*, ETR) and biochemical traits (peroxidases enzymes), resulting in the preservation of metabolic processes and cellular homeostasis. Under increasingly variable and extreme climatic conditions, the development and deployment of new techniques to mitigate the effects of such extreme conditions are vital. Satisfying both the demand for higher yields and the skepticism of advanced genetic manipulation, chemical-based tools to enhance crop production are of great value. Low levels of residual NO, combined with its relatively innocuous effect on plant production processes and storage, make NO a strong candidate for use in the agricultural industry. Our results highlight the central function of NO in plant tissues, as well as several promising physiological and chemical properties that suggest a role in mitigating the effects of stress conditions in plants.

Supplementary Materials: The following are available online at <http://www.mdpi.com/2073-4395/9/8/0412/s1>, Table S1: Amino acids data from soybean plants submitted to two temperatures (25 °C and 40 °C) and two SNP concentrations (0 e 100 µM), Table S2: Carbohydrates, polyols and organic acids data from soybean plants submitted to two temperatures (25 °C and 40 °C) and two SNP concentrations (0 e 100 µM).

Author Contributions: A.C.C., C.M., and R.G.V. designed the research. R.G.V., C.M., F.B.d.S., and P.F.B. conducted the experiments, collected the samples, and performed physiological measurements. F.B.d.S., C.M., and P.F.B. performed the biochemical analysis and analyzed the data. A.A.R. performed the anatomical analyses. P.F.B., D.F., and A.M. performed the metabolic analyses. All authors discussed the data. R.G.V., C.M., and F.B.d.S. wrote the manuscript with contributions from A.M. and D.F. All authors read and approved the manuscript.

Funding: The research was funded by the National Council for Scientific and Technological Development (CNPq, grant nos. 551456/2010-8 and 552689/2011-4), the Goiano Federal Institute of Education, Science, and Technology (IFGoiano-RV, grants no. DPPG 045/2014), Rio Verde campus, and the Foundation for Research Support of the State of Goiás (FAPEG, grant no. DCR 14/2013). A.M. acknowledges the Australian Research Council (FT120100200 and ITRH140100013).

Acknowledgments: C.M., F.B.d.S., and P.F.B. are grateful to the Coordination for the Improvement of Higher Education Personnel (CAPES) and ROS-F to CNPq for scholarships.

Conflicts of Interest: All authors declare no conflicts of interests.

References

- Rose, G.; Osborne, T.; Greatrex, H.; Wheeler, T. Impact of progressive global warming on the global-scale yield of maize and soybean. *Clim. Chang.* **2016**, *134*, 417–428. [[CrossRef](#)]
- Nienaber, J.A.; Hahn, G.L. Engineering and management practices to ameliorate livestock heat stress. In Proceedings of the International Symposium of CIGR Section II “New Trends in Farm Building”, Évora Proceedings Évora: CIGR, 1 CD-ROM 1, Evora, Portugal, 2 May 2004.
- IPCC. Summary for policymakers. In *Climate Change 2014: Impacts, Adaptation, and Vulnerability*; Field, C., Barros, V.R., Dokken, D.J., Mach, K.J., Mastrandrea, M.D., Bilir, T.E., Chatterjee, M., Ebi, K.L., Estrada, Y.O., Genova, R.C., et al., Eds.; Cambridge University Press: Cambridge, UK, 2014; pp. 1–32. Available online: https://www.ipcc.ch/pdf/assessment-report/ar5/syr/AR5_SYR_FINAL_SPM.pdf (accessed on 25 January 2019).
- Ochuodho, T.O.; Lantz, V.A.; Olale, E. Economic impacts of climate change considering individual, additive, and simultaneous changes in forest and agriculture sectors in Canada: A dynamic, multi-regional CGE model analysis. *For. Policy Econ.* **2016**, *63*, 43–51. [[CrossRef](#)]
- Hasanuzzaman, M.; Nahar, K.; Alam, M.M.; Roychowdhury, R.; Fujita, M. Physiological, biochemical, and molecular mechanisms of heat stress tolerance in plants. *Int. J. Mol. Sci.* **2013**, *14*, 9643–9684. [[CrossRef](#)] [[PubMed](#)]
- Puteh, A.B.; ThuZar, M.; Mondal, M.M.A.; Abdullah, N.A.P.B.; Halim, M.R.A. Soybean [*Glycine max* (L.) Merrill] seed yield response to high temperature stress during reproductive growth stages. *Aust. J. Crop Sci.* **2013**, *7*, 1472–1479.
- Kucharik, C.J.; Serbin, S.P. Impacts of recent climate change on wiscons in corn and soybean yield trends. *Environ. Res. Lett.* **2008**, *3*, 034003. [[CrossRef](#)]
- Sicher, R.C. Temperature shift experiments suggest that metabolic impairment and enhanced rates of photorespiration decrease organic acid levels in soybean leaflets exposed to supra-optimal growth temperatures. *Metabolites* **2015**, *5*, 443–454. [[CrossRef](#)] [[PubMed](#)]
- Yang, J.-D.; Yun, J.-Y.; Zhang, T.H.; Zhao, H.-L. Presoaking with nitric oxide donor SNP alleviates heat shock damages in mung bean leaf discs. *Bot. Stud.* **2006**, *47*, 129–136.
- Hasanuzzaman, M.; Nahar, K.; Alam, M.M.; Fujita, M. Exogenous nitric oxide alleviates high temperature induced oxidative stress in wheat (*Triticum aestivum* L.) seedlings by modulating the antioxidant defense and glyoxalase system. *Aust. J. Crop Sci.* **2012**, *6*, 1314–1323.
- Chen, K.; Chen, L.; Fan, J.; Fu, J. Alleviation of heat damage to photosystem II by nitric oxide in fall fescue. *Photosynth. Res.* **2013**, *116*, 21–31. [[CrossRef](#)]
- Laxalt, A.M.; García-Mata, C.; Lamattina, L. The dual role of nitric oxide in guard cells: Promoting and attenuating the ABA and phospholipid-derived signals leading to the stomatal closure. *Front. Plant Sci.* **2016**, *7*, 476. [[CrossRef](#)]
- Boogar, A.R.; Salehi, H.; Jowkar, A. Exogenous nitric oxide alleviates oxidative damage in turfgrasses under drought stress. *S. Afr. J. Bot.* **2014**, *92*, 78–82. [[CrossRef](#)]
- Hossain, K.K.; Nakamura, T.; Yamasaki, H. Effect of nitric oxide on leaf non-photochemical quenching of fluorescence under heat-stress conditions. *Russ. J. Plant Physiol.* **2011**, *58*, 629–633. [[CrossRef](#)]

15. Song, L.; Yue, L.; Zhao, H.; Hou, M. Protection effect of nitric oxide on photosynthesis in rice under heat stress. *Acta Physiol. Plant.* **2013**, *35*, 3323–3333. [[CrossRef](#)]
16. Sousa, D.M.G.; Lobato, E. *Soil Correction and Fertilization of Soybean Crops*; EMBRAPA-CPAC: Planaltina, Brazil, 1996; p. 30. Available online: <https://www.infoteca.cnptia.embrapa.br/infoteca/bitstream/doc/551684/1/cirtec33.pdf> (accessed on 18 January 2019). (In Portuguese)
17. Fehr, W.R.; Caviness, C.E. *Stages of Soybean Development*; Special report, 80; State University of Science and Technology: Ames, Italy, 1977; p. 11.
18. Ferreira, L.C.; Cataneo, A.C.; Remaeh, L.M.R.; Búfalo, J.; Scavroni, J.; Andréo-Souza, Y.; Soares, B.J.A. Morphological and physiological alterations induced by lactofen in soybean leaves are reduced with nitric oxide. *Planta Daninha* **2011**, *29*, 837–847. [[CrossRef](#)]
19. Zhou, B.; Guo, Z.; Xing, J.; Huang, B. Nitric oxide is involved in abscisic acid-induced antioxidant activities in *Stylosanthes guianensis*. *J. Exp. Bot.* **2005**, *56*, 3223–3228. [[CrossRef](#)] [[PubMed](#)]
20. Wellburn, A.R. The spectral determination of chlorophylls *a* and *b*, as well as total carotenoids, using various solvents with spectrophotometers of different resolution. *J. Plant Physiol.* **1994**, *144*, 307–313. [[CrossRef](#)]
21. Heath, R.L.; Packer, L. Photoperoxidation in isolated chloroplasts: I. Kinetics and stoichiometry of fatty acid peroxidation. *Arch. Biochem. Biophys.* **1968**, *125*, 189–198. [[CrossRef](#)]
22. Del Longo, O.T.; Gonzalez, C.A.; Pastori, G.M.; Trippi, V.S. Antioxidant defences under hyperoxygenic and hyperosmotic conditions in leaves of two lines of maize with differential sensitivity to drought. *Plant Cell Physiol.* **1993**, *34*, 1023–1028.
23. Havir, E.A.; Mc Hale, N.A. Biochemical and developmental characterization of multiple forms of catalase in tobacco leaves. *Plant Physiol.* **1987**, *84*, 450–455. [[CrossRef](#)]
24. Nakano, Y.; Asada, K. Hydrogen peroxide is scavenged by ascorbate-specific peroxidase in spinach chloroplasts. *Plant Cell Physiol.* **1981**, *22*, 867–880.
25. Kar, M.; Mishra, D. Catalase, peroxidase, and polyphenoloxidase activities during rice leaf senescence. *Plant Physiol.* **1976**, *57*, 315–319. [[CrossRef](#)] [[PubMed](#)]
26. Bradford, M.N. A rapid and sensitive method for the quantitation of microgram quantities of protein utilizing the principle of protein-dye binding. *Anal. Biochem.* **1976**, *72*, 248–254. [[CrossRef](#)]
27. Popp, M.; Lied, W.; Meyer, A.J.; Richter, A.; Schiller, P.; Schwitte, H. Sample preservation for determination of organic compounds: Microwave versus freeze-drying. *J. Exp. Bot.* **1996**, *47*, 1469–1473. [[CrossRef](#)]
28. Batista, P.F.; Costa, A.C.; Müller, C.; Silva-Filho, R.O.; Silva, F.B.; Merchant, A.; Mendes, G.C.; Nascimento, K.J.T. Nitric oxide mitigates the effect of water deficit in *Crambe abyssinica*. *Plant Physiol. Biochem.* **2018**, *139*, 310–322. [[CrossRef](#)] [[PubMed](#)]
29. Boldizsár, Á.; Simon-Sarkadi, L.; Szirtes, K.; Soltész, A.; Szalai, G.; Keyster, M.; Kocsy, G. Nitric oxide affects salt-induced changes in free amino acid levels in maize. *J. Plant Physiol.* **2013**, *170*, 1020–1027. [[CrossRef](#)] [[PubMed](#)]
30. Misra, A.N.; Vladkova, R.; Singh, R.; Misra, M.; Dobrikova, A.G.; Apostolova, E.L. Action and target sites of nitric oxide in chloroplasts. *Nitric Oxide* **2014**, *39*, 35–45. [[CrossRef](#)] [[PubMed](#)]
31. Parankusam, S.; Adimulam, S.S.; Bhatnagar-Mathur, P.; Sharma, K.K. Nitric oxide (NO) in plant heat stress tolerance: Current knowledge and perspectives. *Front. Plant Sci.* **2017**, *8*, 1582. [[CrossRef](#)] [[PubMed](#)]
32. Lamonte, O.; Courtois, C.; Barbavon, L.; Pugin, A.; Wendehenne, D. Nitric oxide in plants: The biosynthesis and cell signalling properties of a fascinating molecule. *Planta* **2005**, *221*, 1–4. [[CrossRef](#)] [[PubMed](#)]
33. Zhang, J.-H.; Huang, W.-D.; Liu, Y.-P.; Pan, Q.-H. Effects of temperature acclimation pretreatment on the ultrastructure of mesophyll cells in young grape plants (*Vitis vinifera* L. cv. Jingxiu) under cross-temperature stresses. *J. Integr. Plant Biol.* **2005**, *47*, 959–970. [[CrossRef](#)]
34. Acosta-Motos, J.R.; Diaz-Vivancos, P.; Álvarez, S.; Fernández-García, N.; Sánchez-Blanco, M.J.; Hernández, J.A. NaCl-induced physiological and biochemical adaptative mechanisms in the ornamental *Myrtus communis* L. plants. *J. Plant Physiol.* **2015**, *183*, 41–51. [[CrossRef](#)]
35. Palmieri, M.C.; Sell, S.; Huang, X.; Scherf, M.; Werner, T.; Lindermayr, C. Nitric oxide-responsive genes and promoters in *Arabidopsis thaliana*: A bioinformatics approach. *J. Exp. Bot.* **2008**, *59*, 177–186. [[CrossRef](#)] [[PubMed](#)]
36. Laxalt, A.M.; Beligni, M.V.; Lamattina, L. Nitric oxide preserves the level of chlorophyll in potato leaves infected by *Phytophthora infestans*. *Eur. J. Plant Pathol.* **1997**, *103*, 643–651. [[CrossRef](#)]

37. Hayat, S.; Yadav, S.; Alyemini, M.N. Alleviation of salinity stress with sodium nitroprusside in tomato. *Int. J. Veg. Sci.* **2013**, *19*, 164–176. [[CrossRef](#)]
38. Sung, D.-Y.; Kaplan, F.; Lee, K.-J.; Guy, G.L. Acquired tolerance to temperature extremes. *Trends Plant Sci.* **2003**, *8*, 179–187. [[CrossRef](#)]
39. Brestic, M.; Zivcak, M.; Kalaji, H.M.; Carpentier, R.; Allakhverdiev, S.I. Photosystem II thermostability in situ: Environmentally induced acclimation and genotype specific reactions in *Triticum aestivum* L. *Plant Physiol. Bioch.* **2012**, *57*, 93–105. [[CrossRef](#)] [[PubMed](#)]
40. Kramer, D.M.; Avenson, T.J.; Edwards, G.E. Dynamic flexibility in the light reactions of photosynthesis governed by both electron and proton transfer reactions. *Trends Plant Sci.* **2004**, *9*, 349–357. [[CrossRef](#)]
41. Silva, H.C.C.; Asaeda, T. Effects of heat stress on growth, photosynthetic pigments, oxidative damage and competitive capacity of three submerged macrophytes. *J. Plant Interact.* **2017**, *12*, 228–236. [[CrossRef](#)]
42. Kumar, S.; Gupta, D.; Nayyar, H. Comparative response of maize and rice genotypes to heat stress: Status of oxidative stress and antioxidants. *Acta Physiol. Plant.* **2012**, *34*, 75–86. [[CrossRef](#)]
43. Lindermayr, C. Crosstalk between reactive oxygen species and nitric oxide in plants: Key role of S-nitrosoglutathione reductase. *Free Radic. Biol. Med.* **2018**, *122*, 110–115. [[CrossRef](#)]
44. Yun, B.W.; Feechan, A.; Yin, M.; Saidi, N.B.B.; Le Bihan, T.; Yu, M. S-nitrosylation of NADPH oxidase regulates cell death in plant immunity. *Nature* **2011**, *478*, 264–268. [[CrossRef](#)]
45. Kaplan, F.; Kopka, J.; Haskell, D.W.; Zhao, W.; Schiller, K.C.; Gatzke, N.; Sung, D.Y.; Guy, C.L. Exploring the temperature-stress metabolome of Arabidopsis. *Plant Physiol.* **2004**, *136*, 4159–4168. [[CrossRef](#)] [[PubMed](#)]
46. Gray, H.B.; Winkler, J.R. Hole hopping through tyrosine/tryptophan chains protects proteins from oxidative damage. *Proc. Natl. Acad. Sci. USA* **2015**, *112*, 10920–10925. [[CrossRef](#)] [[PubMed](#)]
47. Leonardis, A.M.; Fragasso, M.; Beleggia, R.; Ficco, D.B.M.; Vita, P.; Mastrangelo, A.M. Effects of heat stress on metabolite accumulation and composition, and nutritional properties of durum wheat grain. *Int. J. Mol. Sci.* **2015**, *16*, 30382–30404. [[CrossRef](#)] [[PubMed](#)]
48. Arbona, V.; Manzi, M.; Ollas, C.D.; Gómez-Cadenas, A. Metabolomics as a tool to investigate abiotic stress tolerance in plants. *Int. J. Mol. Sci.* **2013**, *14*, 4885–4911. [[CrossRef](#)] [[PubMed](#)]
49. Galili, G.; Avin-Wittenberg, T.; Angelovici, R.; Fernie, A.R. The role of photosynthesis and amino acid metabolism in the energy status during seed development. *Front. Plant Sci.* **2014**, *5*, 447. [[CrossRef](#)] [[PubMed](#)]
50. James, F.; Brouquisse, R.; Pradet, A.; Raymond, P. Changes in proteolytic activities in glucose-starved maize root tips: Regulation by sugars. *Plant Physiol. Biochem.* **1993**, *31*, 845–856.
51. Herrera-Rodríguez, M.B.; Pérez-Vicente, R.; Maldonado, J.M. Expression of asparagine synthetase genes in sunflower (*Helianthus annuus*) under various environmental stresses. *Plant Physiol. Bioch.* **2007**, *45*, 33–38. [[CrossRef](#)] [[PubMed](#)]
52. Häusler, R.E.; Ludewig, F.; Krueger, S. Amino acids—A life between metabolism and signaling. *Plant Sci.* **2014**, *229*, 225–237. [[CrossRef](#)] [[PubMed](#)]
53. Hildebrandt, T.M.; Nesi, A.N.; Araújo, W.L.; Braun, H.P. Amino acid catabolism in plants. *Mol. Plant* **2015**, *8*, 1563–1579. [[CrossRef](#)]
54. León, J.; Costa, Á.; Castillo, M.C. Nitric oxide triggers a transient metabolic reprogramming in Arabidopsis. *Sci. Rep.* **2016**, *6*, 37945. [[CrossRef](#)]
55. Arasimowicz, M.; Floryszak-Wieczorek, J. Nitric oxide as a bioactive signalling molecule in plant stress responses. *Plant Sci.* **2007**, *172*, 876–887. [[CrossRef](#)]
56. Hu, J.; Yang, H.; Mu, J.; Lu, T.; Peng, J.; Deng, X.; Zuo, J. Nitric oxide regulates protein methylation during stress responses in plants. *Mol. Cell* **2017**, *67*, 702–710. [[CrossRef](#)] [[PubMed](#)]
57. Iglesias, M.J.; Terrile, M.C.; Correa-Aragunde, N.; Colman, S.L.; Izquierdo-Álvarez, A.; Fiol, D.F.; Estelle, M. Regulation of SCFTIR1/AFBs E3 ligase assembly by S-nitrosylation of Arabidopsis SKP1-like1 impacts on auxin signaling. *Redox Biol.* **2018**, *18*, 200–210. [[CrossRef](#)] [[PubMed](#)]
58. Scroggins, B.; Neckers, L. Just say NO: Nitric oxide regulation of Hsp90. *EMBO Rep.* **2009**, *10*, 1093–1094. [[CrossRef](#)] [[PubMed](#)]
59. Livingston, D.P.; Hinch, D.K.; Heyer, A.G. Fructan and its relationship to abiotic stress tolerance in plants. *Cell. Mol. Life Sci.* **2009**, *66*, 2007–2023. [[CrossRef](#)] [[PubMed](#)]

60. Kaya, C.; Sonmez, O.; Aydemir, S.; Ashraf, M.; Dikilitas, M. Exogenous application of mannitol and thiourea regulates plant growth and oxidative stress responses in salt-stressed maize (*Zea mays* L.). *J. Plant Interact.* **2013**, *8*, 234–241. [[CrossRef](#)]
61. López-Gresa, M.P.; Maltese, F.; Bellés, J.M.; Conejero, V.; Kim, H.K.; Choi, Y.H.; Verpoorte, R. Metabolic response of tomato leaves upon different plant–pathogen interactions. *Phytochem. Anal.* **2010**, *21*, 89–94. [[CrossRef](#)]



© 2019 by the authors. Licensee MDPI, Basel, Switzerland. This article is an open access article distributed under the terms and conditions of the Creative Commons Attribution (CC BY) license (<http://creativecommons.org/licenses/by/4.0/>).